International Journal of Fluid Machinery and Systems
Vol. 2, No. 3, July-September 2009

Original Paper

Numerical Prediction of Unsteady Flows through Whole Nozzle-Rotor Cascade Channels with Partial Admission

Yasuhiro Sasao[1], Kazuhiro Monma[1], Tadashi Tanuma[2] and Satoru Yamamoto[1]

[1]Department of Computer and Mathematical Sciences, Tohoku University,
Aramaki-aza Aoba 6-6-01, Aoba-ku, Sendai, Miyagi 980-8579, Japan
[2]Keihin Product Operations, Toshiba Corporation
Yokohama, Kanagawa 230-0045, Japan

Abstract

This paper presents a numerical study for unsteady flows in a high-pressure steam turbine with a partial admission stage. Compressible Navier-Stokes equations are solved by the high-order high-resolution finite-difference method based on the fourth-order compact MUSCL TVD scheme, Roe's approximate Riemann solver, and the LU-SGS scheme. The SST-model is also solved for evaluating the eddy-viscosity. The unsteady two-dimensional flows through whole nozzle-rotor cascade channels considering a partial admission are numerically investigated. 108 nozzle passages with two blockages and 60 rotor passages are simultaneously calculated. The influence of the flange in the nozzle box to the lift of rotors is predicted. Also the efficiency of the partial admission stage changing the number of blockages and the number of nozzles is parametrically predicted.

Keywords: Numerical Study, Steam Turbine, Unsteady Flow, Partial Admission, Nozzle-rotor Cascade Channels

1. Introduction

Steam turbines are used in most of the thermal power plants and the nuclear power plants. The improvement of the steam-turbine performance certainly results in the reduction of the greenhouse gas. Large-scale steam turbines with a nozzle governing system have separated nozzle-blade groups (usually four groups with inlet control valves respectively) for the high pressure first stage (admission stage). For the design condition, valves of the three groups are almost fully opened and one valve of the remaining nozzle group is nearly closed to control the mass flow rate of the turbine system. Also super-critical pressure steam turbines, which were introduced into a number of current coal-fired power generation plants, require a high stiffness design for their admission stage nozzles (nozzle box structure). In these nozzles, some nozzle-blade spacings especially near the horizontal joint flanges are blocked to reinforce their structural stiffness against high pressure and high temperature steam conditions. In these admission stages, since the nozzle-blade spacings are partially opened, the flows into the rotor cascade channels are fluctuated in the circumstantial direction. Generally, internal flows through this kind of partially-opened admission stages cause the loss of the performance. It is also known that this structure causes unsteady and disturbed flows affecting the following rotor blades. The rotor cascade channels occasionally lose flows due to the blocking of the flow at the flange and it results in a relatively lower performance at the admission stage. This loss is called the partial admission loss. Although the prediction of the loss is important, the experimental studies are hard to conduct because of the difficulty of the measurement in actual steam conditions. Therefore, the numerical prediction is quite valuable. But it is suggested that the whole flow fields including nozzles, rotors, and the blocks of the flange and the closed nozzle group should be calculated simultaneously to predict the actual performance. Only a few numerical studies for this flow problem have been reported, because they also require a large-scale computation. A performance prediction for a partial admission has been presented by Cho[1]. He [2] and Sakai [3] have reported the numerical studies solving the quasi three-dimensional Navier-Stokes equations and compared with the experimental results. However, no massive computations such assuming whole nozzle-rotor cascade channels have been reported yet.

Recently our research group has developed computational codes for unsteady flows of wet-steam through 2-D and 3-D multi-stage cascade channels in a steam turbine using the high-order high-resolution finite-difference method [4][5]. In this paper, the 2-D code is applied to unsteady flows in whole nozzle-rotor cascade channels of a partial admission stage. As numerical examples, the unsteady 2-D flows with a partial admission stage in a middle class coal-fired steam turbine are calculated assuming 108 nozzle passages with two blockages and 60 rotor passages. The effect of the blockage to the unsteady force of rotors is numerically predicted. The performance affected by the change of the number of blockages and the number of nozzles is also parametrically predicted.

Received May 25 2009; revised September 1 2009; accepted for publication September 7 2009: Review conducted by Prof. Tong Seop Kim. (Paper number O09015)
Corresponding author: Satoru Yamamoto, Professor, yamamoto@caero.mech.tohoku.ac.jp

2. Fundamental equations

The fundamental equations solved in this study are two-dimensional compressible Navier-Stokes equations and they consist of conservation laws of the mass, the momentums, and the total energy. Also the SST model[6] is solved for the prediction of eddy viscosity. The set of equations in general curvilinear coordinates is written by

$$\frac{\partial Q}{\partial t}+\frac{\partial F_i}{\partial \xi_i}+S+H=0 \qquad (i = 1, 2) \tag{1}$$

where Q, F, S, and H are the vector of unknown variables, vectors of flux, viscous term, and source terms as follows

$$Q=J\begin{bmatrix}\rho\\ \rho u_1\\ \rho u_2\\ e\\ \rho k\\ \rho\omega\end{bmatrix},\quad F_i=J\begin{bmatrix}\rho U_i\\ \rho u_1 U_i+(\partial\xi_i/\partial x_1)p\\ \rho u_2 U_i+(\partial\xi_i/\partial x_2)p\\ (e+p)U_i\\ \rho k U_i\\ \rho\omega U_i\end{bmatrix},\quad S=-J\frac{\partial\xi_i}{\partial x_j}\frac{\partial}{\partial\xi_i}\begin{bmatrix}0\\ \tau_{1j}\\ \tau_{2j}\\ \tau_{kj}u_k+q_j\\ \sigma_{kj}\\ \sigma_{\omega j}\end{bmatrix},\quad H=-J\begin{bmatrix}0\\0\\0\\0\\S_k\\S_\omega\end{bmatrix} \qquad (i = 1, 2) \tag{2}$$

3. Numerical method

The high-order high-resolution finite-difference method based on the fourth-order MUSCL TVD scheme [7] and the Roe's approximate Riemann solver [8] is used for the space discretization of convection terms in Eq.(1). The viscosity term is calculated by the second-order central-difference scheme. The LU-SGS scheme [9] is employed for the time integration.

4. Numerical results

4.1 Computational grid

The schematic of the computational grid is shown in Fig. 1. This grid system has three regions: the nozzle region, the blockage region and the rotor region. The shapes of nozzle and rotor were designed by Toshiba. The nozzle region consists of four nozzles partitioned off each in walls. Each nozzle group consists of 31 or 23 nozzle blades. A modified H-type computational grid with 64x64 grid points is generated for each nozzle blade spacing. Two blockage regions correspond to the flange of the nozzle box. They consist of four H-type computational grids with 24x64 grid points. The rotor region consists of 60 rotor blades. A modified H-type computational grid with 128x64 grid points is generated for each rotor blade. The sum of grid points in all regions is 954,368. Numerical accuracy changing grid points was checked and the present grid could get almost the same results with those using a finer grid. The moving velocity of rotor is calculated from the angular velocity and the diameter at the mid-span of the designed 3-D rotor. The 3-D effect due to centrifugal force and Coriolis force are neglected in this study because of the limitation of the 2-D calculations. The solid wall condition is applied not only on blade surfaces but also on the flow path wall boundaries between 1st Nozzle and 4th Nozzle, 2nd Nozzle and 3rd Nozzle. On all solid surfaces, the flow velocities are set to zero and the adiabatic wall condition for temperature is adopted.

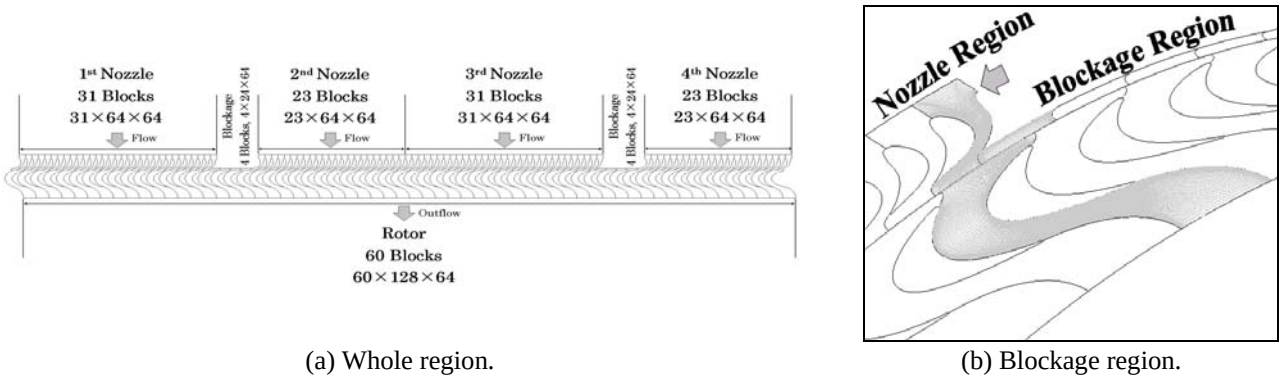

(a) Whole region. (b) Blockage region.

Fig. 1 Computational grids.

4.2 Unsteady flow through partial admission stage

Unsteady flows through the whole nozzle and the rotor cascade channels defined in the previous section are first calculated. The flow initial conditions are that the inlet Mach number is 0.131, the inlet Reynolds number is 1.20×10^8 and the outlet Mach number is 0.185. The working gas is dry steam without wetness.

Figure 2 shows the calculated instantaneous vorticity contours. It is found that the dry steam is strongly disturbed behind the

Received xx xxx 20xx
Corresponding author: Satoru Yamamoto, Professor, yamamoto@caero.mech.tohoku.ac.jp

blockage of the nozzle box. The influence extends to flow fields in rotor cascade channels which have passed through the blockage region. A number of vortices are generated from the near-wall region of the flange and they stream into rotor passages. Totally about eight rotor passages are influenced by the vortical flow. This disturbance is known as the so-called ventilation loss[10].

Figure 3 shows the trace of the calculated non-dimensional tangential force (lift) on one rotor blade while the rotor passes through whole nozzle and blockage regions. The non-dimensional lift C_L^* is defined by

$$C_L^* = \frac{N_L}{A_{rotor} P_0} \tag{3}$$

where P_0 is the stagnation pressure, A_{rotor} is the rotor blade projection area to the tangential direction, and N_L is the tangential component of the lift force. The lift is changing periodically as moving through the nozzle and the blockage regions. Except for the blockage region, the space-averaged value is approximately near 0.002. But, the lift decreases as approaching the blockage region. After the beginning of the blockage region, the lift recovers as approaching the intermediate point in the blockage region. Then, the lift has a positive peak value at the location marked by 'A' as shown in Fig.3. The lift decreases again rapidly toward the end of the blockage region and finally it has a negative peak value at the location 'B'.

Figures 4(a) and 4(b) show the instantaneous static pressure distributions on the rotor blade at the locations A and B. Figures 5(a) and 5(b) show the instantaneous static pressure contours in the flow field when the time is corresponding to that of Figs. 4(a) and 4(b). In Fig. 4(a), a lower pressure peak is found locally on the suction surface. It suggests that a strong vortex passing near the suction side induces the peak value. On the other hand in Fig.4(b), a higher static pressure is observed on the suction surface. In this instantaneous time, the rotor cascade channels, in which the working gas has not been sufficiently supplied due to the flow blockage at the flange, suddenly encounter a high-pressure flow from the nozzles just after the flange. The high-pressure flow through the rotor cascade channels increases pressure on the suction surface as shown in Fig.4(b). The pressure loss is known as the so-called sector-end loss.

Figures 6 and 7 show the instantaneous temperature contours near the 1st nozzle region and the blockage region. The temperature contours in Fig.6 are similarly formed in each nozzle or rotor channel. On the other hand in Fig.7, the instantaneous temperature contours are similarly formed in each nozzle channel. But, those in rotor channels are obviously disturbed due to the sector-end loss. The cyclic disturbances cause non-recoverable momentum and energy exchanges, and leading to an aerodynamic energy loss [2]. The present computational code could get both the ventilation loss and the sector-end loss known as typical losses observed in nozzle-rotor cascade channels with a partial admission. The obtained results suggest that these losses certainly affect the performance of high-pressure steam turbines.

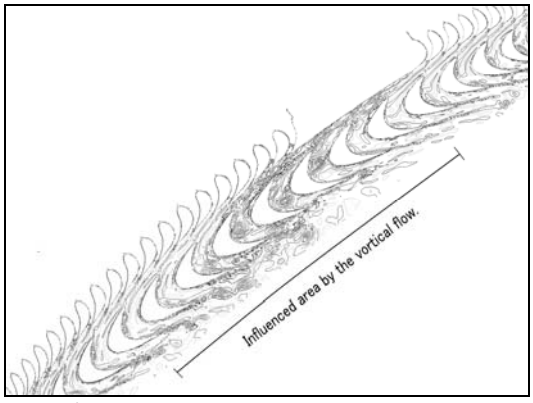

Fig. 2 Instantaneous vorticity contours.

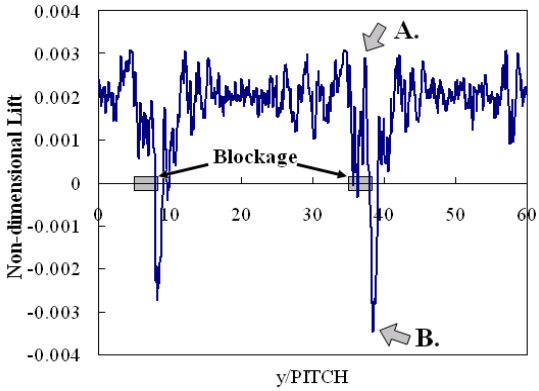

Fig. 3 Trace of non-dimensional lift coefficient on a rotor.

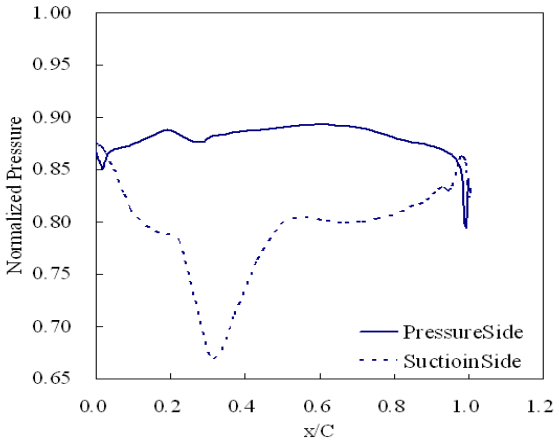

(a) Location A.

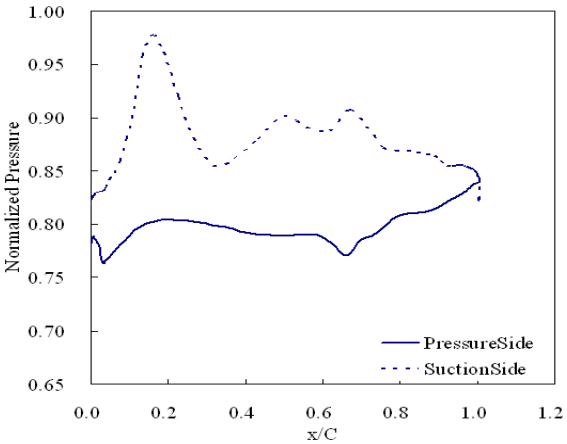

(b) Location B.

Fig. 4 Instantaneous static pressure distributions on the rotor surface.

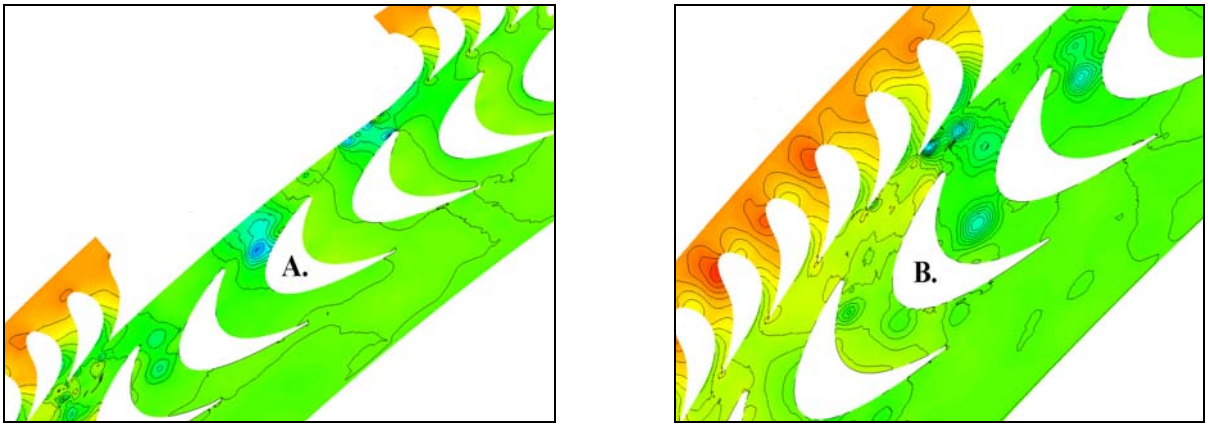

(a) Location A. (b) Location B.

Fig. 5 Instantaneous static pressure contours.

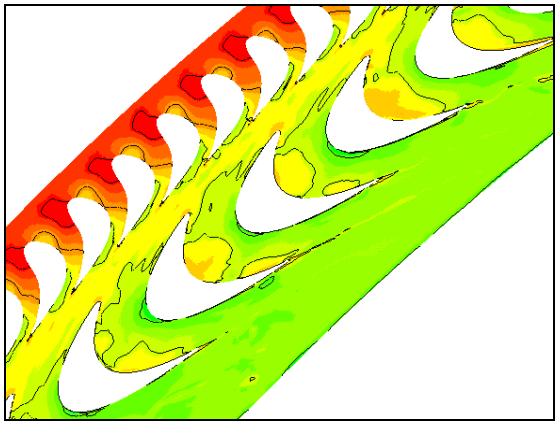

Fig. 6 Instantaneous static temperature contours near 1st nozzle region.

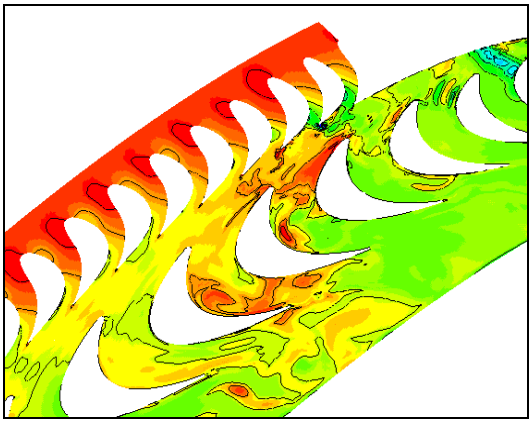

Fig. 7 Instantaneous static temperature contours near the blockage region.

4.3 Performance prediction of partial admission stage

The performance of partial admission stages is parametrically predicted in this section. Figure 8 shows different five configurations for the partial admission stage. Case 1 is the same with the case in the section 4.2. In Case 2, one of four nozzles is assumed to be closed. The location of the closed nozzle is changed in Case 3. Case 4 has 4 blockage regions. Case 5 has 8 blockages regions. The proportion of the total length of the blockage region in whole of nozzle region is equal in any case. The initial flow conditions are that the inlet Mach number is 0.131, the inlet Reynolds number is 1.20×10^8 and the outlet Mach number is 0.185. It should be noticed here that the change of the blockage thickness and the number isn't a realistic approach for the actual design. In this study, the calculations are conducted only to get information how the efficiency is varied by changing the blockage thickness and the number.

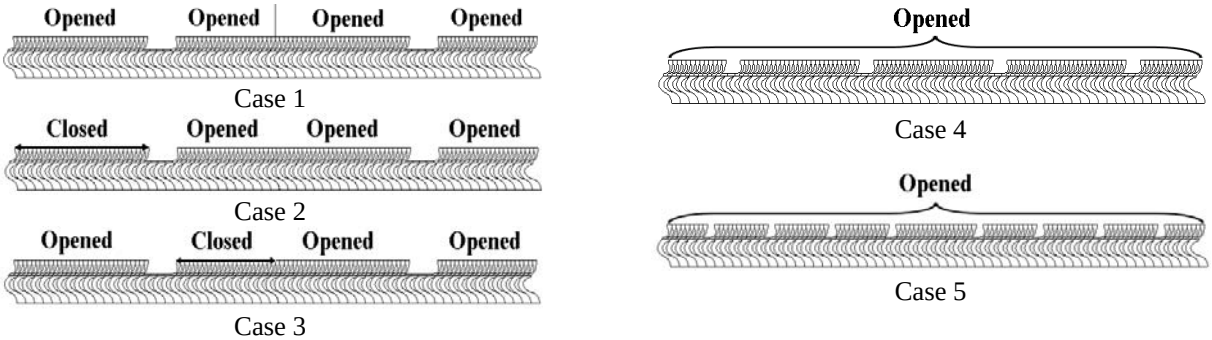

Fig. 8 Schematic of computational grids.

The non-dimensional output ratio and the total-total efficiency are predicted. The total-total efficiency η_{tt} is defined by

$$\eta_{tt} = \frac{h_{t0} - h_{t1}}{h_{t0} - h^*} = \frac{\dfrac{L}{G}}{h_{t0} - h^*} \tag{4}$$

where h_{t0} is the inlet total enthalpy, h_{t1} is the outlet total enthalpy and h^* is the enthalpy of the end state of isentropic expansion calculated from the steam table[11]. G is the total flow rate. The output of turbine L is the total lift work and defined by

$$L = v_{rotation} \times \sum_{n=1}^{60} N_n \tag{5}$$

where v_{rotation} is the rotational speed of rotor, N_n is the tangential component of lift force on n-th rotor.

The calculated output ratios and total-total efficiency ratios are shown in Table 1. The output ratio and total-total efficiency ratio are normalized by the values obtained in Case 1. The output ratios for Case 2 and Case 3 become worse. It is due to the close of one nozzle. On the other hand, those in Case 4 and Case 5 increase. The flow rates in Case 4 and Case 5 were almost the same with that in Case 1. Mass flow rates in Case 4 and Case 5 are almost the same with that in Case 1. But, the total-total efficiency is improved in Case 4 and Case 5 compared with that in Case 1. Consequently, the partial admission in Case 5 gets the best performance in this study. This result indicates that the shortening the length of the flange results in the decrease of the ventilation loss and the sector-end loss.

Figures 9 and 10 show the instantaneous vorticity contours and the trace of the non-dimensional lifts in Case 4 and Case 5. In these cases, the partial admissions in Case 4 and Case 5 keep positive lift values in whole flow fields. No extraordinary negative peak values such in Case 1 is observed. The reason why the efficiency in Case 5 becomes the highest value in all cases is understandable from Fig.10(b).

Table 1 Comparison of performance.

Case No.	**1**	**2**	**3**	**4**	**5**
Num. of cascades	108	77	85	108	108
Output ratio	1.000	0.704	0.784	1.036	1.073
Total-total efficiency ratio	1.000	0.987	0.996	1.036	1.073

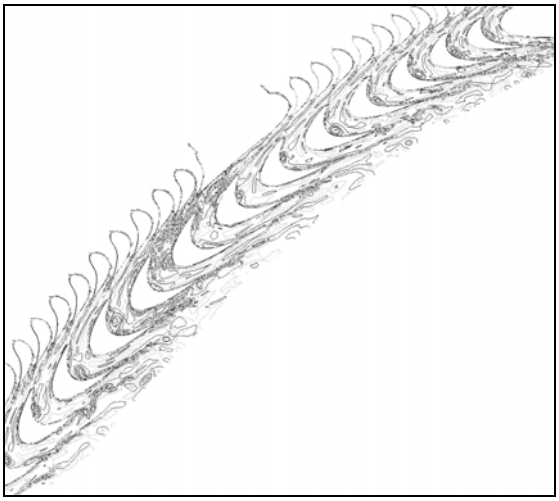

(a) Instantaneous vorticity contours.

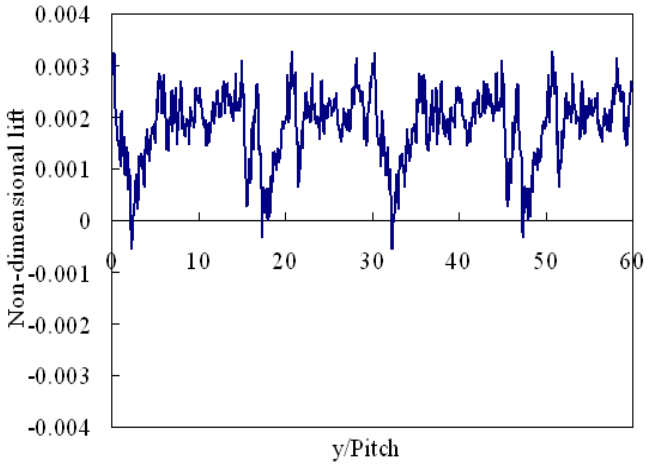

(b) Trace of non-dimensional lift coefficient on a rotor.

Fig. 9 Computational results in Case 4.

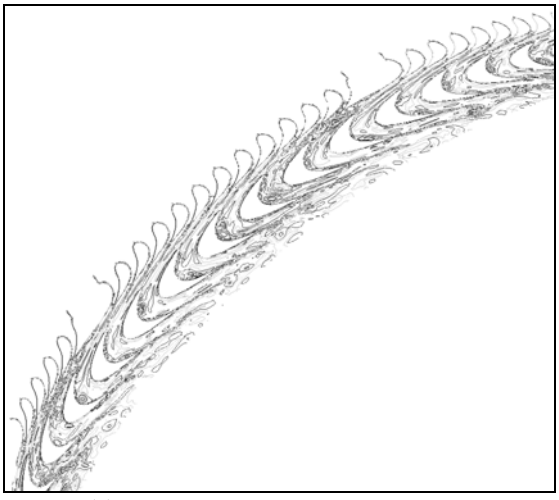

(a) Instantaneous vorticity contours.

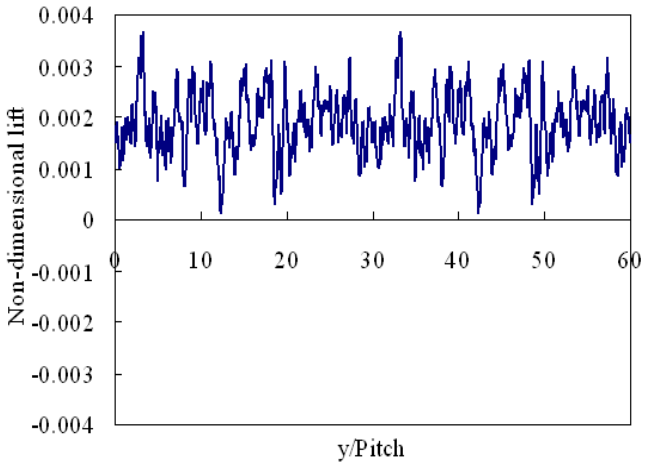

(b) Trace of non-dimensional lift coefficient on a rotor.

Fig. 10 Computational results in Case 5.

5. Conclusion

Unsteady two-dimensional flows through whole nozzle-rotor cascade channels with a partial admission were calculated using the high-order high-resolution numerical method developed by our group. The flow characteristics affected by the blockage region and the rotor performance were numerically investigated. Then, it was found that vortex flows generated near the blockage region stream into the rotor channels and they disturb the flows significantly. The ventilation loss may be induced by the vortical flows in the rotor channels. The flow feature associated with the sector-end loss was also observed in the calculated results. A high-pressure flow from a nozzle cascade channel next to the flange streams into the rotor channels and it induces higher pressure on the suction surface of rotors. Next, the efficiencies changing the number of blockages and closing a part of nozzles were parametrically predicted. In the cases assuming the close of one nozzle, the output ratio got worse. As dividing the blockages, the total-total efficiency was improved. Although two-dimensional flows were assumed in this study, typical flows inducing the ventilation loss and the sector-end loss were successfully captured. Therefore, the present approach will be useful for designing the partial admission stage in high-pressure steam turbines. The three-dimensional computations will be conducted at the next stage of the present study.

Nomenclature

p : Static pressure
u_i : Component of physical velocities
U_i : Component of contravariant velocities
e : Total internal energy per unit volume
k : Turbulent kinetic energy
q_j : Component of heat fluxes
S_k : Source term for k equation
S_ω : Source term for ω equation
t : Physical time
ρ : Density
κ : Laminar heat conductivity coefficient
κ^t : Turbulent heat conductivity coefficient
σ_{kj} : Diffusion term for k equation
$\sigma_{\omega j}$: Diffusion term for ω equation
ξ_i : Component of general curvilinear coordinates
τ_{ij} : Viscous stress tensors
ω : Turbulent specific dissipation rate

References

[1] Cho, S., Cho, C. and Kim, C., 2006, “Performance Prediction on a Partially Small Axial-Type Turbine,” JSME International Journal, Series B, Vol. 49, No. 4, pp. 1290-1297.
[2] He, L., 1997, “Computation of Unsteady Flow through Steam Turbine Blade Rows at Partial Admission,” Proceedings of Institution of Mechanical Engineers, Vol. 211, Part A, pp. 197-205.
[3] Sakai, N., Harada, T. & Imai, Y., 2006, “Numerical Study of Partial Admission Stages in Steam Turbine,” JSME International Journal, Series B, Vol. 49, No. 2, pp. 212-217.
[4] Sasao, Y. and Yamamoto, S., 2005, “Numerical Prediction of Unsteady Flows through turbine Stator-rotor Channels with Condensation,” Proceeding of ASME Fluids Engineering Summer Conference, FEDSM 2005-77205, CD-ROM.
[5] Yamamoto, S., Sasao, Y., Sato S. and Sano K., 2007, “Parallel-Implicit Computation of Three-dimensional Multistage Stator-Rotor Cascade Flows with Condensation,” Proceedings of the 18th AIAA Computational Fluid Dynamics Conference, CD-ROM(paper#4460).
[6] Menter, F.R., 1994, “Two-Equation Eddy-Viscosity Turbulence Models for Engineering Applications,” AIAA Journal, Vol. 32, No. 8, pp. 1598-1605.
[7] Yamamoto, S. and Daiguji H., 1993, “Higher-Order-Accurate Upwind Schemes for Solving the Compressible Euler and Navier-Stokes Equations,” Computers and Fluids, Vol. 22, No. 2/3, pp. 259-270.
[8] Roe, P.L., 1981, “Approximate Riemann Solvers, Parameter Vectors, and Difference Schemes,” Journal of Computational Physics, Vol. 43, pp. 357-372.
[9] Yoon, S. and Jameson, A., 1988, “Lower-upper Symmetric-Gauss-Seidel Method for the Euler and Navier-Stokes Equations,” AIAA Journal, Vol. 26, pp. 1025-1026.
[10] Fridh, J.A., 2002, “Experimental Configuration and Partial Admission,” Technical Report, SNEA Project P12457-2.
[11] IAPWS, 1997, “Release on the IAPWS Formulation 1997 for the Thermodynamic Properties of Water and Steam”.